FEBS Letters 583 (2009) 3317–3322

FEBS Letters

journal homepage: www.FEBSLetters.org

Crystal structure of the NEMO ubiquitin-binding domain in complex with Lys 63-linked di-ubiquitin

Azusa Yoshikawa [a,b], Yusuke Sato [a,b], Masami Yamashita [a,c], Hisatoshi Mimura [a], Atsushi Yamagata [a], Shuya Fukai [a,c,*]

[a] *Structural Biology Laboratory, Life Science Division, Synchrotron Radiation Research Organization and Institute of Molecular and Cellular Biosciences, The University of Tokyo, Tokyo 113-0032, Japan*
[b] *Department of Biological Information, Graduate School of Bioscience and Biotechnology, Tokyo Institute of Technology, Yokohama 226-8501, Japan*
[c] *Department of Medical Genome Sciences, Graduate School of Frontier Sciences, The University of Tokyo, Chiba 277-8501, Japan*

ARTICLE INFO

Article history:
Received 13 August 2009
Revised 14 September 2009
Accepted 14 September 2009
Available online 18 September 2009

Edited by Kaspar Locher

Keywords:
Ubiquitin
IκB kinase
NF-κB
X-ray crystallography
Coiled-coil

ABSTRACT

NEMO is essential for activation of the NF-κB signaling pathway, which is regulated by ubiquitination of proteins. The C-terminal leucine zipper of NEMO and its adjacent coiled-coil region (CC2-LZ) reportedly bind to linear ubiquitin chains with 1 μM affinity and to Lys 63-linked chains with 100 μM affinity. Here we report the crystal structure of the CC2-LZ region of mouse NEMO in complex with Lys 63-linked di-ubiquitin (K63-Ub_2) at 2.7 Å resolution. The ubiquitin-binding region consists of a 130 Å-long helix and forms a parallel coiled-coil dimer. The Ile 44-centered hydrophobic patch of ubiquitin is recognized in the middle of the NEMO ubiquitin-binding region. NEMO interacts with each K63-Ub_2 *via* a single ubiquitin-binding site, consistent with low affinity binding with K63-Ub_2.

Structured summary:
MINT-7262681: *NEMO* (uniprotkb:O88522) *binds* (MI:0407) to *Ubiquitin* (uniprotkb:P62991) by *pull down* (MI:0096)
MINT-7262667: *Ubiquitin* (uniprotkb:P62991) and *NEMO* (uniprotkb:O88522) *bind* (MI:0407) by *X-ray crystallography* (MI:0114)

1. Introduction

NF-κB signaling is a central pathway that regulates gene expression in inflammatory and immune responses. Signaling from various stimuli converges on the IκB kinase (IKK) complex, which phosphorylates IκB, a cytosolic inhibitor of NF-κB [1]. Phosphorylated IκB is subsequently modified with polyubiquitin chains linked by means of Lys 48 that signal its proteasomal degradation, resulting in translocation of NF-κB to the nucleus and the activation of its target genes. The IKK complex contains two catalytic subunits, IKKα and IKKβ, and one regulatory subunit IKKγ or NEMO (*N*F-κB *e*ssential *mo*dulator) [2]. Although NEMO has no intrinsic kinase activity, IKK activation requires NEMO [3]. In the canonical TNF-α stimulated pathway for NF-κB activation, recruitment and activation of IKK downstream of TNF-R1 require the receptor interacting protein (RIP) that is modified with polyubiquitin chains linked by means of Lys 63, which are structurally and functionally distinct from the abovementioned Lys 48-linked chains [4]. After TNF-α stimulation, RIP is co-immunoprecipitated with NEMO and the Lys 63-linked polyubiquitinated RIP is detected as multiple bands when analyzed by SDS–PAGE [4,5]. At the inception of our work, NEMO appeared to interact with Lys 63-linked polyubiquitin chains on RIP to enable transduction of a signal from activated TNF-R1 to the IKK complex, resulting in NF-κB activation. However, recent studies showed that NEMO interacts with linear ubiquitin chains [6–8], and may be modified with linear chains by the LUBAC E3 ligase [9].

NEMO is a multidomain protein with a molecular mass of 50 kDa. The domain composition of NEMO includes two coiled-coils (termed as CC1 and CC2), a leucine zipper (LZ) and a C-terminal zinc finger (ZF). Although the three-dimensional structure of the full-length NEMO has not yet been solved, partial structures show that NEMO is mostly α-helical [6,7,10,11]. The CC1 region interacts with the IKK C-terminal tails [10]. The CC2-LZ region of NEMO has been reported to interact with Lys 63-linked and linear polyubiquitin chains and to be modified by linear and Lys 63-linked ubiquitin

* Corresponding author. Address: Structural Biology Laboratory, Life Science Division, Synchrotron Radiation Research Organization and Institute of Molecular and Cellular Biosciences, The University of Tokyo, Tokyo 113-0032, Japan. Fax: +81 3 5841 7807.
E-mail address: fukai@iam.u-tokyo.ac.jp (S. Fukai).

0014-5793/$36.00 © 2009 Federation of European Biochemical Societies. Published by Elsevier B.V. All rights reserved.
doi:10.1016/j.febslet.2009.09.028

chains [6–9,12]. The ZF region has been also reported to interact with ubiquitin [13]. The CC2-LZ ubiquitin-binding region of NEMO shares several conserved or functionally equivalent residues with ABIN proteins (ABIN-1, -2 and -3) and optineurin, which have been suggested to bind Lys 63-linked polyubiquitin chains [14–16]. Optineurin has been previously proposed to negatively regulate TNFα-induced NF-κB activation by competing with NEMO for Lys 63-linked polyubiquitinated RIP [16]. Further, binding of ABIN-1 to Lys 63-linked polyubiquitin chains may prevent TNF-induced programmed cell death in vivo [14]. These reports suggested that Lys 63-linked ubiquitin-chain binding by NEMO-related proteins could be a generally important theme in TNF-stimulated NF-κB signaling. However, our work and several recent reports call into question the relevance of NEMO•Lys 63-linked chains interactions and suggest that instead NEMO may interact with linear ubiquitin chains. The functional relevance of this distinction is currently unclear.

We report the crystal structure of the mouse NEMO ubiquitin-binding domain in complex with Lys 63-linked di-ubiquitin (K63-Ub_2) at 2.7 Å resolution. The structure of the complex reveals a single ubiquitin-binding site where the Ile 44-centered hydrophobic patch of either the distal or proximal ubiquitin moiety was recognized by NEMO and is consistent with data suggesting that this portion of NEMO does not specifically bind Lys 63-linked polyubiquitin chains.

2. Materials and methods

2.1. Sample preparation

The gene encoding mouse NEMO (249–343) was PCR amplified and cloned into pCold-GST expression vector (GE Healthcare) with NdeI and XhoI sites to produce the N-terminal GST fusion protein. *Escherichia coli* Rosetta™ (DE3) cells (Invitrogen) were transformed with the expression vector, and cultured in LB media containing 100 mg/L ampicillin at 37 °C. When the optical density at 600 nm of the culture reached ~0.5, the culture was incubated for 30 min at 15 °C. Thereafter, isopropyl-β-D-thiogalactopyranoside (IPTG) was added to a final concentration of 0.3 mM to induce protein expression for 17 h at 15 °C. Cells were collected by centrifugation at 8000×*g* for 15 min, and were disrupted by sonication in phosphate buffered saline (PBS) containing 1 mM dithiothreitol (DTT) and 1 mM phenylmethylsulfonyl fluoride (PMSF). The lysates were centrifuged at 30 000×*g* for 60 min, and the supernatants were loaded onto a Glutathione Sepharose FF column (GE Healthcare) pre-equilibrated with PBS containing 1 mM DTT. The column was washed with PBS containing 1 mM DTT. The GST fused proteins were eluted with 50 mM Tris–HCl buffer (pH 8.0) containing 150 mM NaCl, 1 mM DTT and 15 mM reduced glutathione, and were diluted with two volumes of 50 mM Tris–HCl buffer containing 1 mM DTT. The samples were loaded onto a ResourceQ anion exchange column (GE Healthcare) and were eluted with a linear gradient of 0–1 M NaCl. The GST tags were cleaved by PreScission protease (GE Healthcare), and the samples were dialyzed against 50 mM Na-phosphate buffer (pH 6.0) and 1 mM DTT. The proteins were loaded onto a ResourceS cation exchange column (GE Healthcare) and were eluted with a linear gradient of 0-1 M NaCl. The eluted samples were loaded onto a Superdex200 16/60 (prep grade) column (GE Healthcare) pre-equilibrated with 10 mM Tris–HCl buffer (pH 7.2) containing 50 mM NaCl and 5 mM β-mercaptoethanol.

2.2. Crystallization

K63-Ub_2 was prepared as described previously [17]. The purified mouse NEMO (249–343) was concentrated to 10 g/L by using an Amicon Ultra-15 10 000 MWCO filter (Millipore), following the manufacturers' instructions. Initial crystallization screening in the presence of twofold molar excess of K63-Ub_2 was performed using the sitting drop vapor diffusion method at 20 °C, with a Mosquito® liquid-handling robot (TTP Lab Tech). We tested about 500 conditions, using crystallization reagent kits supplied by Hampton Research, and initial hits were further optimized. The best crystals of the NEMO (249–343)•K63-Ub_2 complex were obtained at 20 °C with the sitting drop vapor diffusion method by mixing 1 μL of protein solution with an equal amount of precipitant solution containing 0.2 M ammonium acetate, 20% PEG3350, and 0.1 M HEPES-Na (pH 7.0) and allowed to equilibrated against 0.5 mL of reservoir solution containing 0.2 M ammonium acetate, 14% PEG3350, and 0.1 M HEPES-Na (pH 7.0). The crystal of the NEMO (249–343)•K63-Ub_2 complex, which was used for the final structure refinement, belong to the space group $P2_1$, with the unit cell parameters, a = 55.4 Å, b = 45.9 Å, c = 83.3 Å, β = 99.8°. The selenomethionine (SeMet)-labeled NEMO (249–343) was prepared in the same way as the native NEMO (249–343), except that NEMO (249–343) was overproduced in the methionine-auxotroph *E. coli* strain, B834 (DE3), which was cultured in Core™ medium (Wako) with 30 mg/L L-selenomethionine (Nakalai Tesque).

2.3. Structure determination

The crystals of the NEMO (249–343)•K63-Ub_2 complex were cryo-protected by 20% glycerol. Diffraction data sets were collected at 90 K in the beamline BL41XU of SPring-8 (Hyogo, Japan) and NW12A of PF-AR (Tsukuba, Japan) and processed with HKL2000 [18] and the CCP4 program suite [19]. MOLREP was used to solve the structure of the NEMO (249–343)•K63-Ub_2 complex by molecular replacement [20]. The crystal structure of ubiquitin (PDB ID 1UBQ) was used as a search model. Atomic models were built by using either COOT [21] or O [22] with careful inspection. Positions of the methionine residues in NEMO were confirmed by an anomalous difference Fourier map generated from SAD dataset of the Se-Met-labeled NEMO (249–343)•K63-Ub_2 complex crystal. Refinement was carried out by using CNS [23] with iterative correction and refinement of the atomic models. The final models have excellent stereochemistry and R_{free} values of 0.292 for the NEMO (249–343)•K63-Ub_2 complex at 2.7 Å resolution. Data collection, phasing, and refinement statistics are shown in Table 1. All molecular graphics were prepared with PyMOL (DeLano Scientific; http://www.pymol.org). The coordinates and structure factors of mouse NEMO CC2-LZ in complex with K63-Ub_2 have been deposited in the Protein Data Bank with accession codes 3JSV.

3. Results and discussion

3.1. Structural overview

We crystallized residues 249–343 of mouse NEMO in the presence of enzymatically synthesized K63-Ub_2 [17] and collected a diffraction data set which extends to d_{min} = 2.7 Å resolution. The crystal structure was solved by molecular replacement using a mono-ubiquitin structure (PDB ID: 1UBQ) [24] as a search model. A SAD data set was also collected from a Se-Met labeled crystal to confirm the positions of Met 288 residues in mouse NEMO by an anomalous difference Fourier map. The ubiquitin-binding region of the K63-Ub_2-bound mouse NEMO consists of a 130-Å long α helix and forms a parallel coiled-coil dimer (Fig. 1), similar to that of human NEMO alone and of mouse NEMO in complex with linear Ub_2 [6,7]. The asymmetric unit contains two NEMO monomers that form a parallel coiled-coil and one molecule of K63-Ub_2. The coiled-coil structure of the NEMO ubiquitin-binding region is pseudo-twofold symmetrical and ubiquitin moieties bind

Table 1
Data collection and refinement statistics.

Data collection	
X-ray source	SPring8 BL41XU
Wavelength (Å)	1.0000
Space group	$P2_1$
Unit cell parameter	a = 55.4 Å, b = 45.9 Å c = 83.3 Å, β = 99.8°
Resolution (Å)	50.0–2.70 (2.75–2.70)
Unique reflections	11 492
Total reflections	358 746
Completeness (%)	98.8 (97.9)
$I/\sigma(I)$	14.2 (3.8)
R_{sym}	0.066 (0.216)
Refinement	
Number of atoms: protein, water	2740, 63
Rmsd bond length (Å)	0.007
Rmsd bond angle (°)	1.2
Average B factors (Å^2): protein, water	81.6, 54.1
Residues in core region (%)	91.5
Residues in additionally allowed region (%)	8.5
Residues in generously allowed region (%)	0.0
Residues in disallowed region (%)	0.0
R_{work}, R_{free}	0.250, 0.294

The numbers in parentheses are for the highest resolution shell.
$R_{sym} = \Sigma|I_{avg} - I_i|/\Sigma I_i$.
$R_{cullis} = \Sigma||\mathbf{F}_{PH} - \mathbf{F}_P| - |\mathbf{F}_{H(calc)}||/\Sigma|\mathbf{F}_{PH}|$.
$R_{work} = \Sigma|F_o - F_c|/\Sigma F_o$ for reflections of working set.
$R_{free} = \Sigma|F_o - F_c|/\Sigma F_o$ for reflections of test set (5% of total unique reflections).

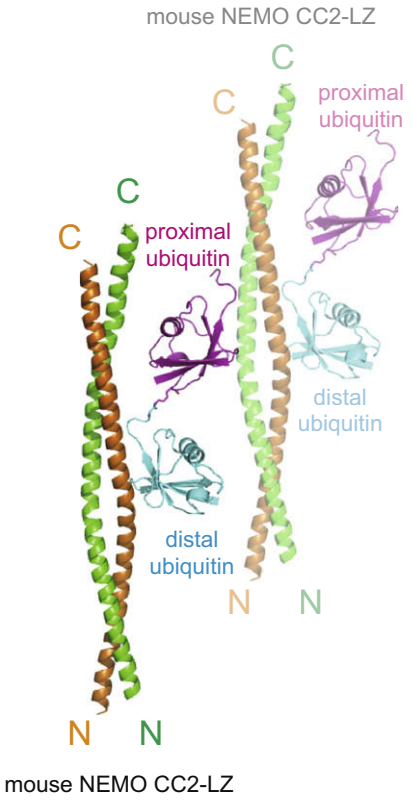

Fig. 1. Crystal structure of CC2-LZ region of mouse NEMO in complex with K63-Ub_2. NEMO monomers interacting with the distal and proximal ubiquitin moieties are colored orange and green, respectively. The distal and proximal ubiquitin moieties are colored cyan and magenta, respectively.

to both sides of the NEMO homodimer in the crystal. Unexpectedly, K63-Ub_2 simultaneously binds with regions containing residues 293–308 in the two distinct coiled-coil dimers of NEMO (Fig. 1). In the crystal, the distal ubiquitin moiety interacts with one side of the NEMO coiled-coil with a buried surface area of 1214 Å^2, whereas the proximal ubiquitin moiety interacts with the other side with a buried surface area of 1141 Å^2. The observed difference in buried surface is likely caused by the different conformation of the C-terminal tails of the distal and proximal ubiquitin moieties.

3.2. Interactions with K63-Ub_2

The Ile 44-centered hydrophobic patch is of general importance for ubiquitin recognition [25]. NEMO recognizes this hydrophobic patch on the distal and proximal ubiquitin moieties of K63-Ub_2 (Fig. 2). The recognition of both ubiquitin moieties in the NEMO•K63-Ub_2 complex is similar to that of the distal ubiquitin moiety in the NEMO•linear Ub_2 complex (Fig. 2) [6]. The middle region of the NEMO ubiquitin-binding region (*i.e.* residues 293–308 of mouse NEMO) is accommodated in the concave surface formed by Leu 8, Ile 44, His 68, Val 70 and Arg 72 of ubiquitin (Fig. 2a and c). Leu 8 and Ile 44 in ubiquitin and Val 293 and Ala 296 in mouse NEMO are interleaved with each other. Val 70 of ubiquitin is sandwiched between Ile 300 and Gln 297 in mouse NEMO. Our NEMO•K63-Ub_2 complex lack a hydrogen bond between Glu 289 of NEMO and His 68 of ubiquitin, which is observed in the NEMO•linear Ub_2 complex [6]. The C-terminal tail region of the distal ubiquitin is also recognized by NEMO (Fig. 2b), where two sequence specific hydrogen bonds are observed: The Nη and Nε atoms of Arg 72 and Arg 74 in ubiquitin hydrogen bond with the Oδ and Oε atoms of Asp 304 and Glu 308 in mouse NEMO, respectively. Further, Leu 73 of the distal ubiquitin intercalates between the aromatic rings of NEMO residues Tyr 301 in one helix and Phe 305 in the other helix. On the other hand, the conformation of the C-terminal tail of the proximal ubiquitin is different from that of the distal ubiquitin (Fig. 2b and d). The lack of an isopeptide linkage from Gly 76 in the proximal ubiquitin allows side-chain conformations of Arg 72 and Arg 74 of ubiquitin, which are different from those in the distal ubiquitin moiety and disrupt hydrogen bonds between ubiquitin Arg 72 and NEMO Asp 304 and between ubiquitin Arg 74 and NEMO Glu 308.

3.3. Comparison with the NEMO–K63-Ub_2 interacting mode observed in solution

Recently, Wu and her colleagues reported the crystal structure of the human NEMO CC2-LZ region [7]. They also specified amino acid residues crucial for the interactions between human NEMO and ubiquitin by NMR and pull-down analyses. Most of the NEMO mutations that drastically impaired the ubiquitin binding (*i.e.* Val 293 [300], Ile 300 [307], Tyr 301 [308], Asp 302 [309], Phe 305 [312], Glu 308 [315] of mouse NEMO [human NEMO]) are involved in ubiquitin binding in our crystal structure of the NEMO•K63-Ub_2 complex. These residues are conserved or replaced by functionally equivalent residues in the NEMO-related proteins, optineurin and ABIN proteins (ABIN-1, -2 and -3) (Fig. 3). Also, our structure is consistent with the essentially identical patterns of chemical shift perturbation and peak broadening in the course of NEMO titration for K63-Ub_2 species containing ^{15}N-labeled distal or proximal ubiquitin moieties. Leu 8, Ile 44, His68 and Val 70 of both proximal and distal ubiquitin moieties, which they identified as key residues for the interaction, are recognized by NEMO in our structure. Further, Arg 312 of mouse NEMO (corresponding to Arg 319 of human NEMO) and Thr 12 of ubiquitin, which are crucial for linear Ub_2 recognition but not for K63-Ub_2 recognition, are not involved in the NEMO–K63-Ub_2 interaction in the present complex. Thus the NEMO–ubiquitin interactions that are detected by NMR and pull-down analyses can be mostly explained by our NEMO•K63-Ub_2

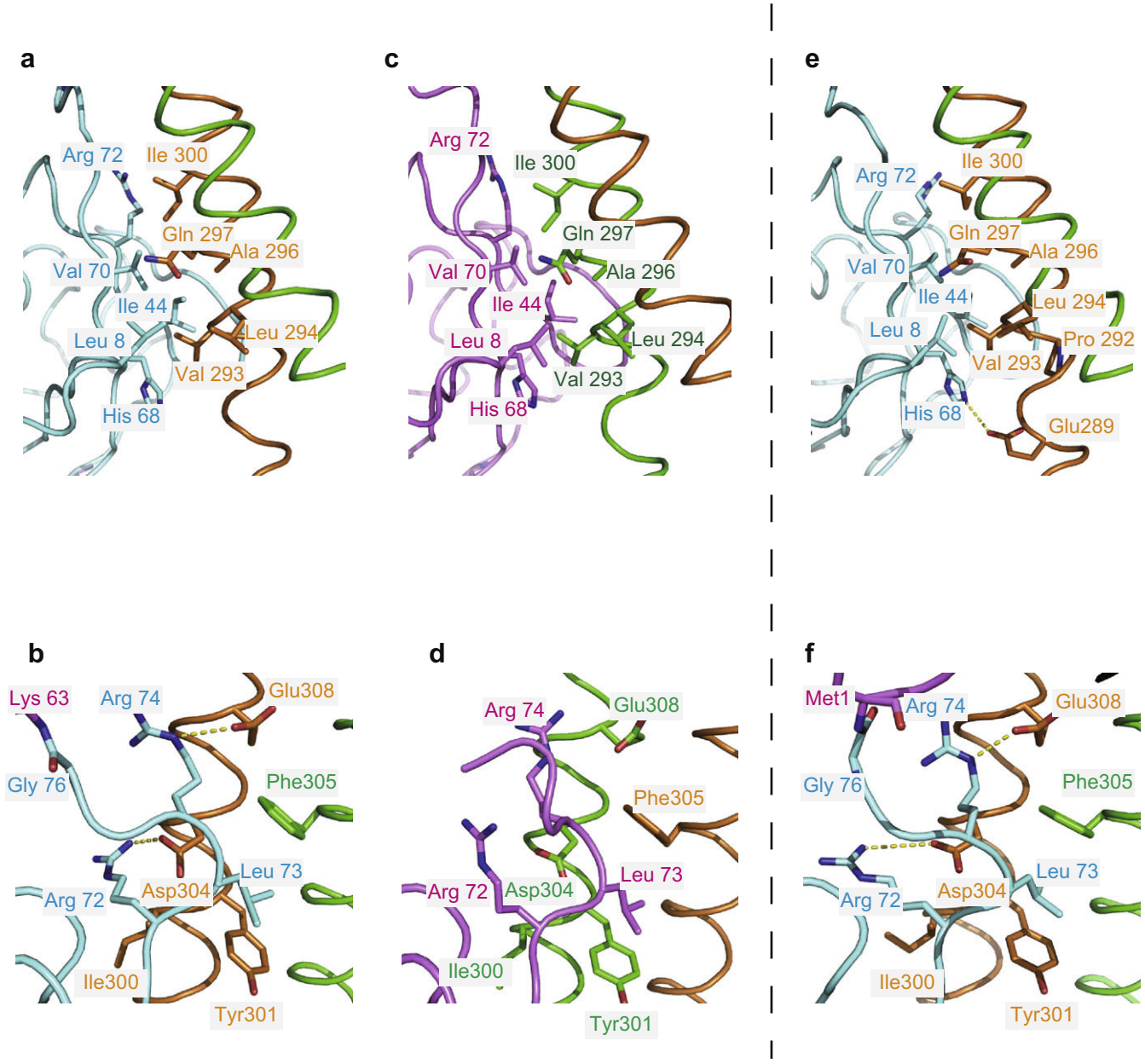

Fig. 2. Interactions between NEMO CC2-LZ region and di-ubiquitin. Coloring schemes are the same as Fig. 1. (a) Interactions with the body of the distal ubiquitin of K63-Ub_2. (b) Interactions with the tail of the distal ubiquitin of K63-Ub_2. (c) Interactions with the body of the proximal ubiquitin of K63-Ub_2. (d) Interactions with the tail of the proximal ubiquitin of K63-Ub_2. (e) Interactions with the body of the distal ubiquitin of linear Ub_2. (f) Interactions with the tail of the distal ubiquitin of linear Ub_2.

complex structure, although we do not observe a direct interaction of mouse NEMO Val 316 (corresponding to Ala 323 of human NEMO) with ubiquitin. Wu and her colleagues predicted the simultaneous binding of the proximal and distal ubiquitin moieties to the front and back sides of a single NEMO dimer, like a hand gripping on a rope in a U-shaped manner. However, their predicting docking mode is implausible, since the distal and proximal ubiquitin moieties bound to NEMO from both sides in the crystal could not be connected through the Lys 63-linked isopeptide linkage even if drastic conformational changes in the Lys 63 side chain of the proximal ubiquitin and the C-terminal tail of the distal ubiquitin could occur. Therefore, we conclude that the binding of K63-Ub_2 to two distinct NEMO dimers, as is observed in the crystal, could potentially occur in solution, although the interaction between NEMO and the proximal ubiquitin moiety may be weakened by the lack of the hydrogen bonds described above.

3.4. Linkage preference and implications on the mechanism for the activation of the IKK complex

Recent reports showed that NEMO itself is modified with linear polyubiquitin chains by the ubiquitin ligase complex LUBAC [9] and that NEMO interaction with linear ubiquitin chains is important for NF-κB activation [6]. Actually, isothermal titration calorimetry (ITC) estimated the K_d values of the NEMO–linear Ub_2 and NEMO–K63-linked Ub_2 interactions to be 1.4 μM and 131 μM, respectively [6,7]. Our GST-pull-down experiment also showed that mouse NEMO CC2-LZ selectively binds to linear Ub_2 (Supplementary Fig. S1). This low affinity interaction between NEMO and K63-Ub_2 is consistent with a single-site binding of K63-Ub_2 to NEMO shown in our NEMO•K63-Ub_2 complex structure.

Dikic and his colleagues proposed two plausible activation mechanisms for IKKβ activation by transautophosphorylation

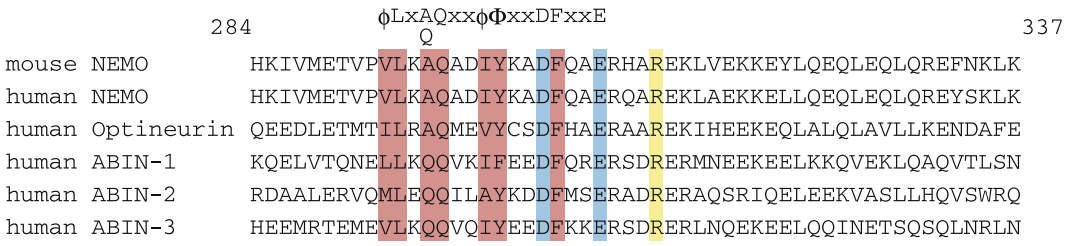

Fig. 3. Amino acid sequence alignment of NEMO and NEMO-related proteins. Residues involved in hydrophobic and hydrophilic interactions with ubiquitin are highlighted in magenta and cyan, respectively. Arginine residue that was suggested to be involved in linear ubiquitin interaction is highlighted in yellow.

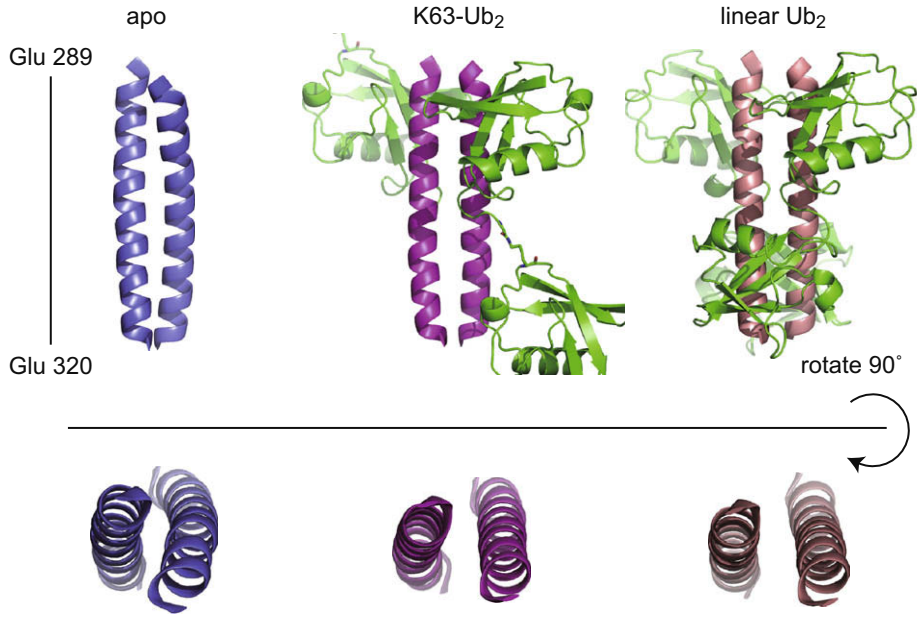

Fig. 4. Comparison among the apo, K63-Ub_2-bound, and linear Ub_2-bound NEMO structures. The apo, K63-Ub_2-bound, and linear Ub_2-bound NEMO CC2-LZ regions are colored blue, magenta, and pink, respectively. The bound Ub_2 are colored in green.

[6,26]: First, clustering and oligomerization of the IKK complex facilitated by ubiquitination or ubiquitin binding may activate IKKβ *in trans*. Second, IKKβ may be activated after a conformational change in the IKK complex. In the second scenario, it was postulated that structural changes in NEMO are translated to IKKβ resulting in transphosphorylation and subsequent activation of IKKβ. This scenario seems to be supported by the observed conformational change in the coiled-coil region of NEMO induced by binding with linear Ub_2 [6]. This conformational change in the NEMO coiled-coil may affect the conformation of the IKK binding region of NEMO. Intriguingly, the conformation of the NEMO coiled-coil region in our NEMO•K63-Ub_2 complex is similar to that in the NEMO•linear Ub_2 complex (Fig. 4), suggesting that binding of the distal ubiquitin to NEMO may primarily induce the conformational change in the coiled-coil region of NEMO. Since NEMO can reportedly bind with Lys 63-linked tetra-ubiquitin with weaker affinity than linear Ub_2, Lys 63-linked ubiquitin chains might be able to activate IKK through a conformational change in the NEMO coiled-coil region. Although our structure supports a notion that linear ubiquitin chains are the primary substrate for NEMO, further studies will be required to provide a clear answer about the roles of Lys 63-linked chains for the IKK activation.

Acknowledgements

We thank C. Toyoshima for support of this research. We thank S. Kaiser for critical reading and improvement of this manuscript. We are grateful to K. Iwai for providing us with reagents for the overexpression of E1, E2-25K and linear Ub_2. We are grateful to M. Komada for providing us with the overexpression vectors of ubiquitin mutants for K63-Ub_2 and K48-Ub_2 synthesis. We thank the beam-line staffs at NW12A of Photon Factory (Tsukuba, Japan) and BL41XU of SPring8 (Hyogo, Japan) for technical help during data collection. This work was supported by Grants from MEXT to S.F., A. Ya, and H.M., Y.S. and M.Y. are supported by JSPS research fellowships for young scientists.

Appendix A. Supplementary data

Supplementary data associated with this article can be found, in the online version, at doi:10.1016/j.febslet.2009.09.028.

References

[1] Hayden, M.S. and Ghosh, S. (2008) Shared principles in NF-κB signaling. Cell 132, 344–362.
[2] Miller, B.S. and Zandi, E. (2001) Complete reconstitution of human IκB kinase (IKK) complex in yeast. Assessment of its stoichiometry and the role of IKKγ on the complex activity in the absence of stimulation. J. Biol. Chem. 276, 36320–36326.
[3] Courtois, G., Smahi, A. and Israel, A. (2001) NEMO/IKKγ: linking NF-κB to human disease. Trends Mol. Med. 7, 427–430.
[4] Zhang, S.Q., Kovalenko, A., Cantarella, G. and Wallach, D. (2000) Recruitment of the IKK signalosome to the p55 TNF receptor: RIP and A20 bind to NEMO (IKKγ) upon receptor stimulation. Immunity 12, 301–311.

[5] Legler, D.F., Micheau, O., Doucey, M.A., Tschopp, J. and Bron, C. (2003) Recruitment of TNF receptor 1 to lipid rafts is essential for TNFα-mediated NF-κB activation. Immunity 18, 655–664.
[6] Rahighi, S. et al. (2009) Specific recognition of linear ubiquitin chains by NEMO is important for NF-κB activation. Cell 136, 1098–1109.
[7] Lo, Y.C., Lin, S.C., Rospigliosi, C.C., Conze, D.B., Wu, C.J., Ashwell, J.D., Eliezer, D. and Wu, H. (2009) Structural basis for recognition of diubiquitins by NEMO. Mol. Cell 33, 602–615.
[8] Ivins, F.J., Montgomery, M.G., Smith, S.J., Morris-Davies, A.C., Taylor, I.A. and Rittinger, K. (2009) NEMO oligomerization and its ubiquitin-binding properties. Biochem. J. 421, 243–251.
[9] Tokunaga, F. et al. (2009) Involvement of linear polyubiquitylation of NEMO in NF-κB activation. Nat. Cell. Biol. 11, 123–132.
[10] Rushe, M. et al. (2008) Structure of a NEMO/IKK-associating domain reveals architecture of the interaction site. Structure 16, 798–808.
[11] Bagneris, C., Ageichik, A.V., Cronin, N., Wallace, B., Collins, M., Boshoff, C., Waksman, G. and Barrett, T. (2008) Crystal structure of a vFlip-IKKγ complex: insights into viral activation of the IKK signalosome. Mol. Cell 30, 620–631.
[12] Wu, C.J., Conze, D.B., Li, T., Srinivasula, S.M. and Ashwell, J.D. (2006) Sensing of Lys 63-linked polyubiquitination by NEMO is a key event in NF-κB activation. Nat. Cell. Biol. 8, 398–406.
[13] Cordier, F., Vinolo, E., Veron, M., Delepierre, M. and Agou, F. (2008) Solution structure of NEMO zinc finger and impact of an anhidrotic ectodermal dysplasia with immunodeficiency-related point mutation. J. Mol. Biol. 377, 1419–1432.
[14] Oshima, S. et al. (2009) ABIN-1 is a ubiquitin sensor that restricts cell death and sustains embryonic development. Nature 457, 906–909.
[15] Wagner, S. et al. (2008) Ubiquitin binding mediates the NF-κB inhibitory potential of ABIN proteins. Oncogene 27, 3739–3745.
[16] Zhu, G., Wu, C.J., Zhao, Y. and Ashwell, J.D. (2007) Optineurin negatively regulates TNFα-induced NF-κB activation by competing with NEMO for ubiquitinated RIP. Curr. Biol. 17, 1438–1443.
[17] Sato, Y. et al. (2008) Structural basis for specific cleavage of Lys 63-linked polyubiquitin chains. Nature 455, 358–362.
[18] Otwinowski, Z. and Minor, W. (1997) Processing of X-ray diffraction data collected in oscillation mode. Meth. Enzymol. 276, 307–326.
[19] Collaborative Computational Project, Number 4 (1994) The CCP4 Suite: Programs for Protein Crystallography. Acta Crystallogr. D Biol. Crystallogr. 50, 760–763.
[20] Vagin, A. and Teplyakov, A. (1997) MOLREP: an automated program for molecular replacement. J. Appl. Crystallogr. 30, 1022–1025.
[21] Emsley, P. and Cowtan, K. (2004) Coot: model-building tools for molecular graphics. Acta Crystallogr. D Biol. Crystallogr. 60, 2126–2132.
[22] Jones, T.A., Zou, J.Y., Cowan, S.W. and Kjeldgaard, M. (1991) Improved methods for binding protein models in electron density maps and the location of errors in these models. Acta Crystallogr. A 47, 110–119.
[23] Brunger, A.T. et al. (1998) Crystallography & NMR system: a new software suite for macromolecular structure determination. Acta Crystallogr. D Biol. Crystallogr. 54, 905–921.
[24] Vijay-Kumar, S., Bugg, C.E. and Cook, W.J. (1987) Structure of ubiquitin refined at 1.8 A resolution. J. Mol. Biol. 194, 531–544.
[25] Hurley, J.H., Lee, S. and Prag, G. (2006) Ubiquitin-binding domains. Biochem. J. 399, 361–372.
[26] Hacker, H. and Karin, M. (2006) Regulation and function of IKK and IKK-related kinases. Sci. STKE 2006, re13.